Jour. of the KGS, Vol. 20, No. 2. March 2004, pp. 5~13

Settlement Characteristics of the Reinforced Railroad Roadbed with Crushed Stones Under a Simulated Train Loading

모사 열차하중 재하에 따른 쇄석강화노반의 침하특성

Hwang, Seon-Keun[1] 황 선 근

요 지

기존의 흙을 사용하여 건설된 철도 노반은 반복적인 교통하중의 증가, 열차속도의 향상, 노반상으로의 지하수의 유입, 노반의 배수능력 저하 등의 이유로 인해 시간경과에 따라 쉽게 그 기능을 상실할 수 있다. 본 연구에서는 실대형시험과 수치해석을 수행함으로써 철도노반으로서의 쇄석강화노반의 성능을 평가하였다. 쇄석강화노반의 탄·소성 연직변위는 모사열차하중의 재하횟수에 관계없이 일반 흙노반에 비해 작은 응답특성을 보였으며, 동일한 노반 부설두께에서는 노반반력계수의 증가에 따라 감소하며, 동일한 강성인 경우 노반 부설두께 증가에 따라 감소하는 경향을 보였다. 하지만, 쇄석강화노반의 부설두께에 비해 노반의 강성이 궤도에 발생하는 전체 소성 연직변위에 더욱 큰 영향을 미치는 것으로 평가되었다.

Abstract

Conventional railroad roadbeds constructed with soils can easily deteriorate with time due to the increase of repeated traffic loading, increase of train speed, built-up of ground water on the roadbed and decrease of permeability in the roadbed layer, etc. In this study, performance of reinforced railroad roadbeds with the crushed stones was investigated through the real scale roadbed tests and numerical analysis. It was found that the reinforced roadbed with crushed stone had less elastic and plastic vertical displacement(settlement) than general soil roadbed regardless of the number of loading cycles. It was also found through the actual testing that for the roadbed with the same thickness, the displacement of reinforced roadbed decreases with the increase of subgrade reaction modulus. The settlement of reinforced roadbed with the same subgrade reaction modulus also decreases with the increase of thickness of the reinforced roadbed. However, the subgrade reaction modulus is a more important factor to the total plastic displacement of the track than the thickness of the crushed stone roadbed.

Keywords : Crushed stones, Reinforced roadbed, Settlement, Subgrade reaction modulus, Vertical displacement

1. Introduction

The reinforced roadbed has the ability to spread out the load intensity on to the subgrade of track structure as well as to prevent the softening of subgrade by providing appropriate stiffness in the roadbed, thus fully supports the track structures. The bearing capacity and durability of roadbed are generally degraded with the duration of usage due to the train loads, freezing and thawing, rainfall and mud pumping phenomenon, etc. It is necessary to develop a reinforced roadbed design system for the Korean railroad environment as a

1 Member, Chief Researcher, Korea Railroad Research Institute (skhwang@krri.re.kr)

countermeasure for the upgrading the speed of train and the safety improvement. There are several different design methods developed and used in the practice to improve the bearing capacity and to elongate the lifetime of track structures. Especially, the reinforcement method utilizing the material with high durability as a roadbed is widely used. However, one should consider the functional and economical aspects as well as characteristics of site specific conditions for the construction of reinforced roadbed.

The performance of the reinforced roadbeds with the crushed stones was investigated through the real scale roadbed tests. Several real scale roadbeds were constructed in the laboratory with different subgrade conditions and tested with the estimated train loads including the impact loading of train.

2. Material and Experimental Procedures

2.1 Tests Materials and Loading System

A weathered granite soil and the crushed stone (MS-40) were chosen as the roadbed construction materials. The particle size distribution curve and compaction curve of each material were shown in Figs. 1(a) and (b). The physical properties of test materials were summarized in Table 1.

The special pit (W×D×L: 5m×3m×22m) for real scale railway roadbed test was constructed in order to build several models with different conditions. The loading system mainly consists of a mobile loading frame, two loading actuators and control system. The loading system (Fig. 2) can cover most of wheel loads of trains in service lines in Korea.

Table 1. Physical properties of test materials

Test Items		Weathered Granite Soil	Crushed Stone
Sieve Analysis	D_{10} (mm)	0.16	0.8
	C_u	11.87	13.5
	C_g	0.96	2.35
	% *Passing* # 200 *Sieve*	12	-
Specific Gravity	G_s	2.59	2.70
Compaction	γ_{dmax} (kN/m^3)	17.1	24.02
	w_{opt}(%)	11.3	7.65

2.2 Test Conditions and Construction of Model Tracks

A clean sand layer of 20cm was placed at the bottom of the pit for drainage purpose. Weathered granite soil layer of 30cm thick was placed on the top of the sand layer and compacted with a vibrating roller compactor to obtain the required condition of roadbed and this process was continued until whole subgrade layer is completed. The plate bearing test was performed to check the bearing capacity of subgrade and the desired subgrade conditions of K_{30}=70MN/m^3 and 110MN/m^3 were achieved.

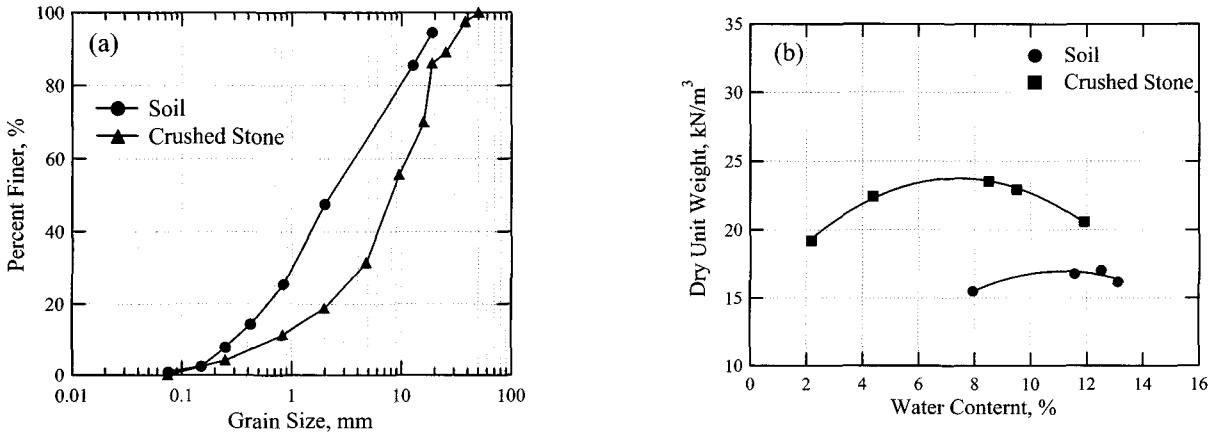

Fig. 1. Particle size distribution curves (a) and compaction curves (b) for roadbed materials

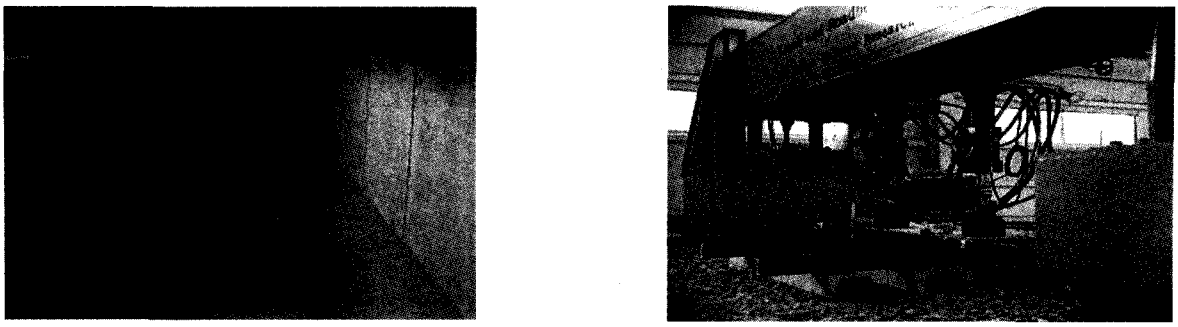

(a) (b)

Fig. 2. Pit for real scale test (a) and loading system (b)

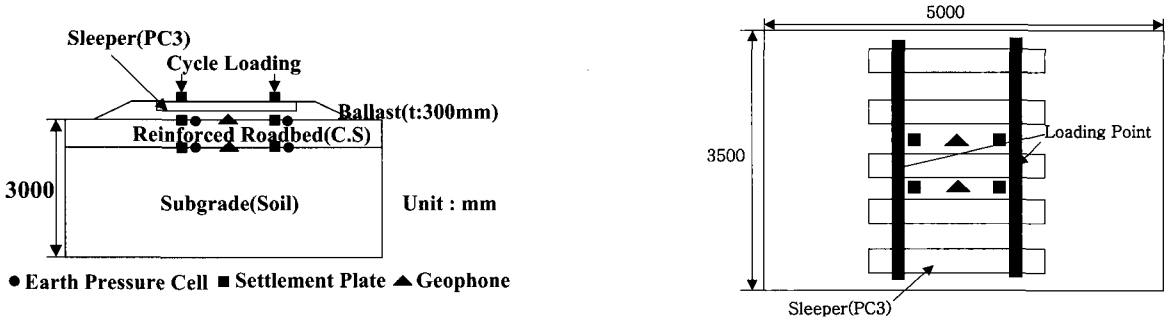

(a) (b)

Fig. 3. Plane (a) and Sectional (b) View of Real Scale Roadbed

The crushed stone and weathered granite soil were used as the reinforced roadbed materials and the thickness of both reinforced roadbeds was 30cm, 50cm and 80cm. The ballast layer of 30cm was then placed on top of the roadbed. The track was 5m(W)×3m(L) in size and consisted of 5 sleepers and 2 rails. The plane and sectional view of real scale model was shown in Fig. 3.

A total of 5 sections were constructed with different conditions as shown in Table 2. In order to monitor the behavior of rail, ballast layer, roadbed and subgrade, several sensors, 8 displacement sensors with settlement plates, 4 velocity sensors (geophone) and 4 earth pressure cells were installed at each model section.

Table 2. Test condition of real scale roadbeds

Test ID	Coeff. of Subgrade Reaction Modulus (MN/m^3)	Thickness of Roadbed(cm)	Roadbed Material
K7d80	70	80	crushed stone
K11d80	110	80	crushed stone
K11d50	110	50	crushed stone
K11d30	110	30	crushed stone
Soil	110	30	weathered granite soil

3. Assessment of Magnitude and Frequency of Loading

The magnitude of loading for real-scale railroad roadbed tests was estimated based on Eq. (3). In general, the roadbed stress should be estimated considering track structure, wheel load, train speed, etc. The tests were carried out under the assumption that continuously welded rail is installed on the straight line section, and the design speed of train is 200km/hr and the design train load is LS-22. Impact factor was calculated as 1.6 using Eq. 2. The magnitude of cyclic loading was estimated using Eq. 3 considering standard loading and the standard deviation of impact factor.

$$S_p = 0.5 \times P_{st} \times (i-1) \quad (1)$$

$$i = 1 + 0.3\frac{V}{100} \quad (2)$$

$$P_w = P_{st} + S_p \quad (3)$$

Where, S_p: standard deviation, P_{st}: static load(= 110kN = half of LS-22 load), i: impact factor(= 1.6), V: train speed(= 200km/hr in this study) and P_w: wheel load(= cyclic load).

The minimum and maximum of sinusoidal cyclic loading were 10kN and 143kN, respectively. For the compaction and stabilization of the ballast layer, 500 cycles of cyclic loading with 0.5Hz of loading frequency were applied on each rail sleeper before the actual cyclic loading test. The loading frequency was calculated as follows:

$$T = \frac{d}{V} \tag{4}$$

Where, T: train-passing time(sec), d: distance between the bogie of train and V: train speed.

Since loading frequency(f) is equal to $\frac{1}{T}$, it becomes $\frac{V}{d}$.

$$f = \frac{1}{T} = \frac{V}{d} \tag{5}$$

The calculated loading frequency for this study is 5Hz and the actual data from several sensors installed in the model track were shown in Fig. 4.

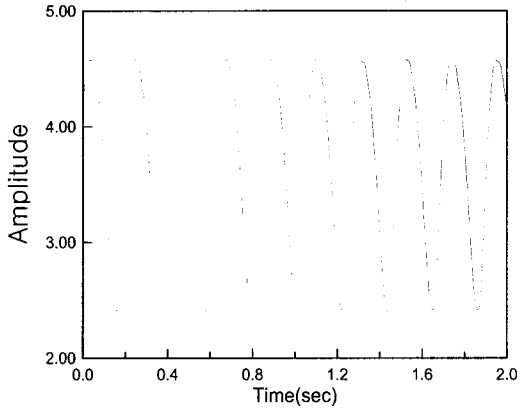

(a) Displacement

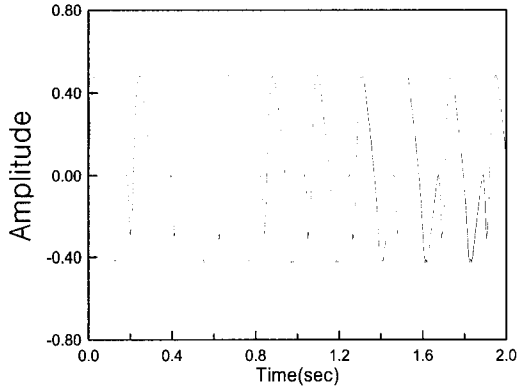

(b) Particle Velocity

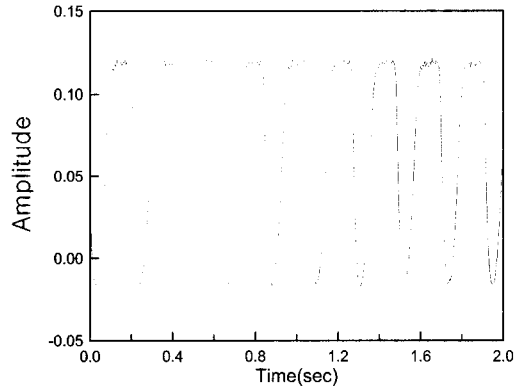

(c) Earth Pressure

Fig. 4. Typical Data Obtained in the Model Test

4. Test Results and Analysis

4.1 Plate Bearing Test

Plate bearing test was carried out on top of the

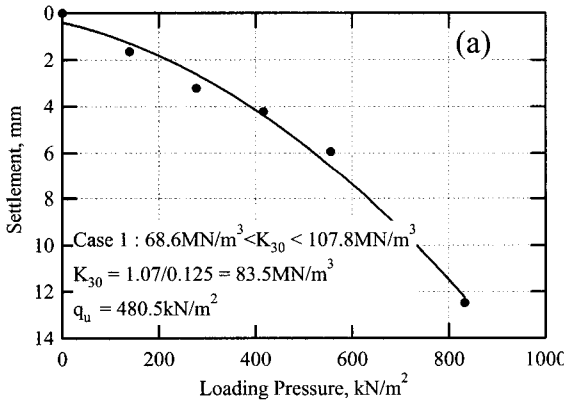

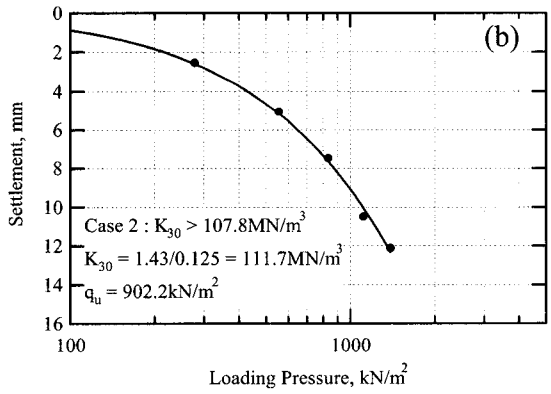

Fig. 5. Typical Result of Plate Bearing Test on the Subgrade

subgrade for each section of model track to confirm if the desired condition was achieved. The reaction modulus of subgrade was obtained using either load-settlement or log(load)-settlement relationship as shown in Fig. 5. The resulting subgrade reaction moduli of all sections were satisfactorily well within the desired condition.

4.2 Load and Displacement Distribution

Track consisted of 5 sleepers which are different with field condition as shown in Fig. 6(b). Comparison between the track used in this study with actual field track was performed with the help of FEM analysis. Stress distribution and displacement upon cyclic loading were shown in Figs. 6(a), (b) and (c).

As it can be seen in Fig. 6(c), there was almost no difference in stress distribution under the sleepers except for the third sleeper from the center sleeper, whereas, the displacement at the outer end of track shows difference in its magnitude due to discrepancy in their end conditions. The actual differences in magnitude was however very small and the effect on the test result was considered to be negligible.

The displacement distribution under the concentrated cyclic loading was investigated to confirm the widely used practice, i.e., 40% at the sleeper of concentrated loading, 20% at the sleepers next to the center sleeper and 10% at the second sleepers from the center sleeper. The actual measured displacement distribution shown in Figs. 7 and 8 reveals that greater displacements occurred at the sleeper #2, 3 and 4, while less displacement occurred at the sleeper # 1 and 5. This result was not

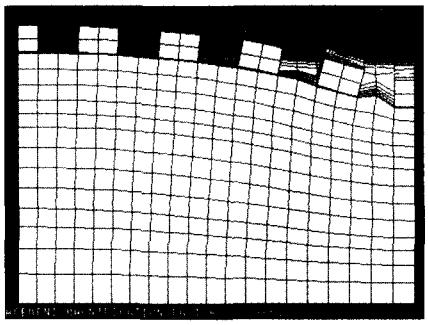

(a) Original Track

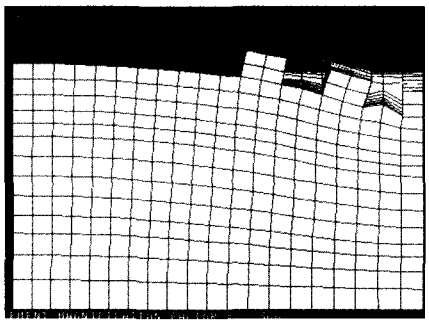

(b) Real Scale Model

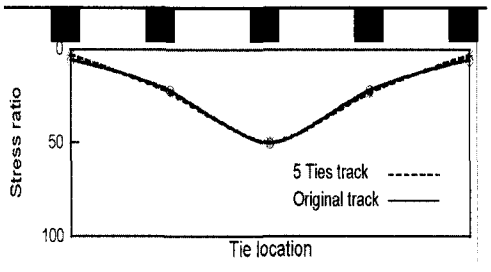

(c) Stress Distribution

Fig. 6. Displacement and Stress Distribution Under the Sleeper for 2 Different Track Conditions

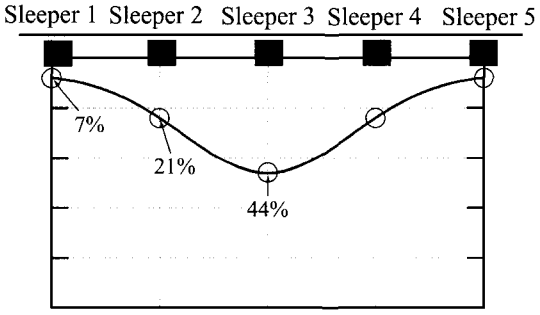

Fig. 7. Displacement Distribution Curve Measured in the Cyclic Loading Test

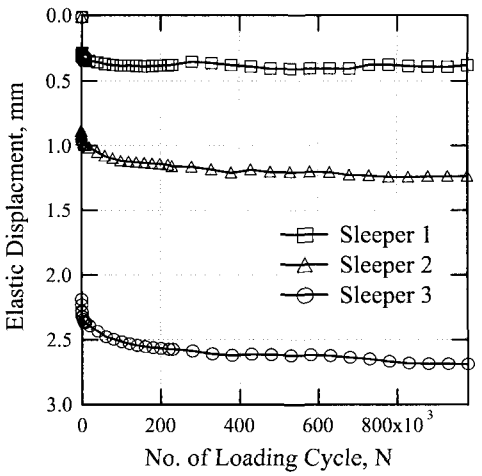

Fig. 8. Changes in the Elastic Displacement at Each Sleeper Locations During the Cyclic Loading

much different from the widely used distribution ratio and the differences were mainly due to the usage of 5 sleeper for testing.

4.3 Elastic and Plastic Displacement

The measurement was periodically performed during the cyclic loading such that each continuous measurement contains at least 25 cycles of loading period. The peak to peak displacement under the cyclic loading was considered as the elastic displacement, whereas the absolute mean value of cyclic displacement from the datum at the beginning of the test was considered as the cumulative plastic displacement (Fig. 9).

The crushed stone roadbed and weathered granite soil roadbed with the same condition (i.e., thickness: 30cm, subgrade reaction modulus: 107.8MN/m^3) was statically tested, and the maximum static displacements at each surfaces were compared in Fig. 10.

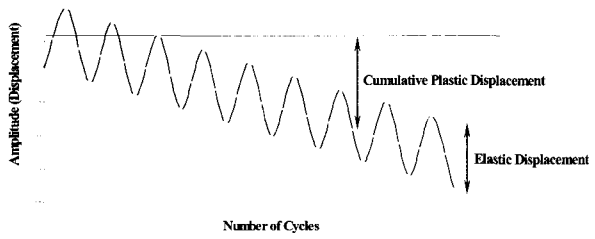

Fig. 9. Definition of Elastic and Plastic Displacement

The displacements at the rail and roadbed surface of crushed stone roadbed were smaller than that of soil roadbed as expected. The magnitude of difference in displacement was greater at the surface of the rail since it is a cumulative displacement of whole section.

It is also interesting to see in Fig. 11 that the percentages of displacement at the roadbed and subgrade surface of both roadbeds sections relative to that of rail surface are almost identical to each other.

The plastic displacements of both roadbed sections after the one million cycles of loading were compared in Fig. 12. It can be seen that the absolute displacements at the rail surface of both roadbeds section were greater than that of static test result shown in Fig. 10. It is obvious that the main reason is the number of loading cycles. The fact that displacements at the surface of roadbeds, however, has no difference with that of Fig. 10 could be explained by the stress concentration at the upper layer.

The relationship between the plastic, elastic displacement and number of loading cycles for both roadbed sections was shown in Figs. 11(a) and (b). It is clearly shown in Figs. 11(a) and (b) that the plastic and elastic displacements of crushed stone roadbed section were always less than that of weathered granite soil roadbed section.

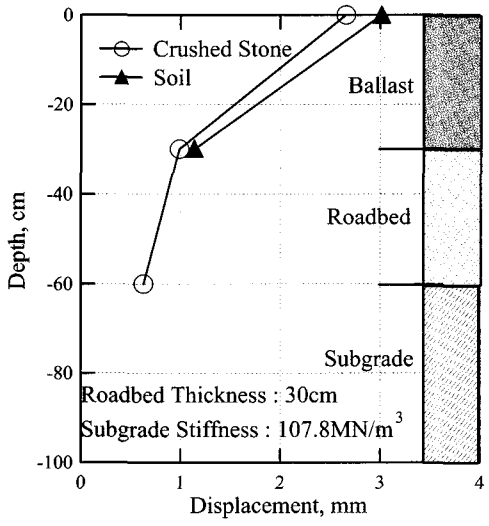

Fig. 10. Comparison of Displacement at Each Surface of Crushed Stone and Soil Roadbed Section

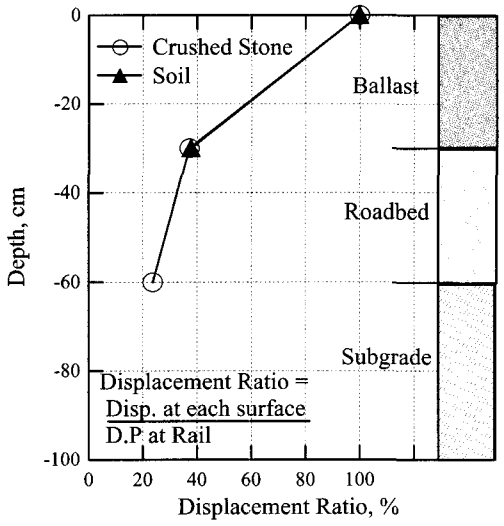

Fig. 11. Distribution of Displacement at the Roadbed and Subgrade Surface of Both Roadbed Sections

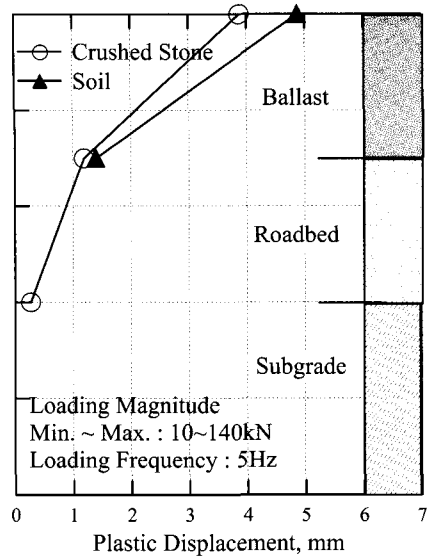

Fig. 12. Comparison of Plastic Displacements of Both Roadbed Sections after one million Cycles of Loading

It is also interesting to see the plastic displacement at the roadbed surface of both roadbed sections occurs rapidly at initial loading stage and converges to certain values after approximately 200 thousand loading cycles. The trend of plastic displacement at the rail surface of both roadbed sections is very similar through out the entire loading cycles. The same explanation of trend as mentioned above can be used to the elastic displacement of both roadbed sections as shown in Fig. 13(b).

4.4 Effect of Roadbed Thickness on Displacement

The effect of roadbed thickness on the static displacement of each layer is shown in Figs. 14(a) and (b). The static displacement at each layer decreases with the increase of roadbed thickness. The magnitude of dis-

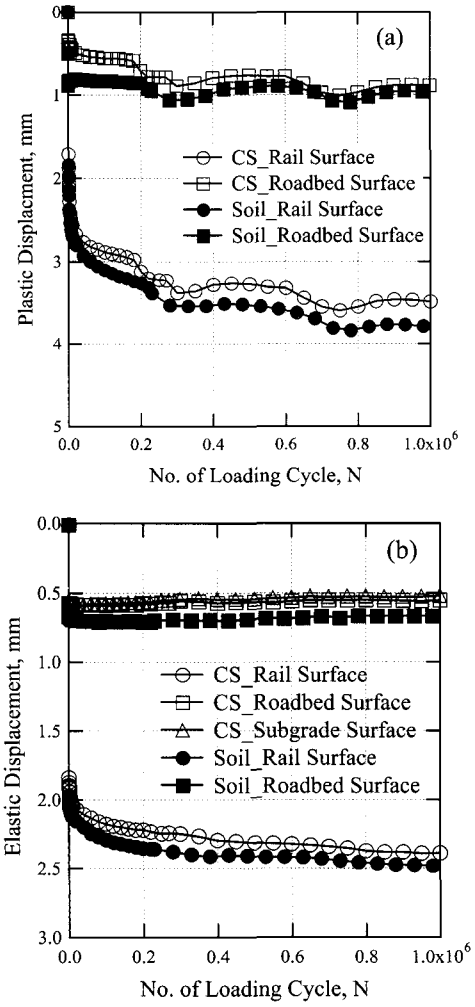

Fig. 13. Relationship Between the Plastic (a), Elastic (b) Displacement and Number of Loading Cycles for Both Roadbed Sections

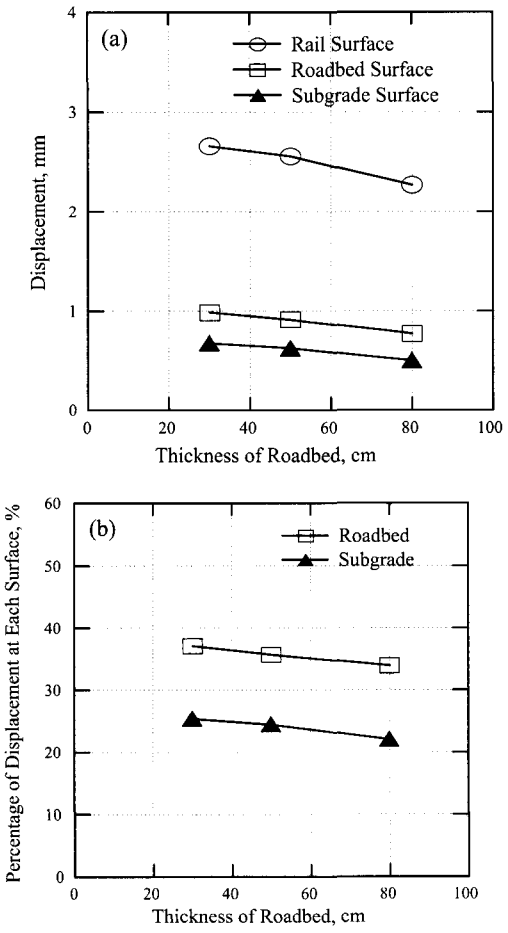

Fig. 14. Relationship Between the Roadbed Thickness and the Static Displacement of the Crushed Stone Roadbed Section

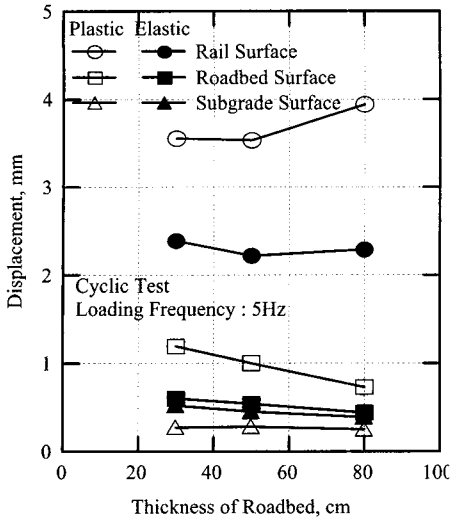

Fig 15. Relationship Between the Roadbed Thickness and the Plastic and Elastic Displacement of the Crushed Stone Roadbed Section

placement in the ballast layer is largest in the ballast layer and smallest in the roadbed layer. The percentages of displacement in the roadbed and subgrade section relative to the total displacement were 33%~37% and 22%~26%, respectively.

The plastic and elastic displacement after one million cycles of loading was shown in Fig. 15. The effect of roadbed thickness on the plastic and elastic displacement indicates that the magnitude of displacement in the roadbed layer tends to decrease with the increase of the thickness of roadbed. In case of the test section with 80cm thick roadbed, however, the ballast layer was so poorly prepared that the measured displacements turn out to be unreasonably greater than expected. The magnitude of plastic and elastic displacements of the subgrade layer was so small (i.e., less than 1mm in all cases) that it is very difficult to confirm any general trend.

In order to check the difference in the displacement of roadbed with different stiffness, cumulative plastic and elastic displacement of two crushed stone roadbeds (K^{30} = 68.6 and 107.8MN/m^3 with 80cm thick layer) was compared in Fig. 16.

The displacement up to 10 thousands cycles of loading could be considered as the displacement in the ballast layer. The displacement after 10 thousands cycles of loading could be considered as the displacement occurring in the roadbed and subgrade layers.

The final elastic and plastic displacement was 3.0mm and 4.9mm for the subgrade reaction modulus with K_{30}= 68.6MN/m^3 and 2.3mm and 4.0mm for the subgrade reaction modulus with K_{30}=107.8MN/m^3. Therefore, with the result of measurement data analysis, the subgrade reaction modulus has more influence on whole displacement than the thickness of roadbed.

5. Conclusions

In this study, characteristics of crushed stone reinforced

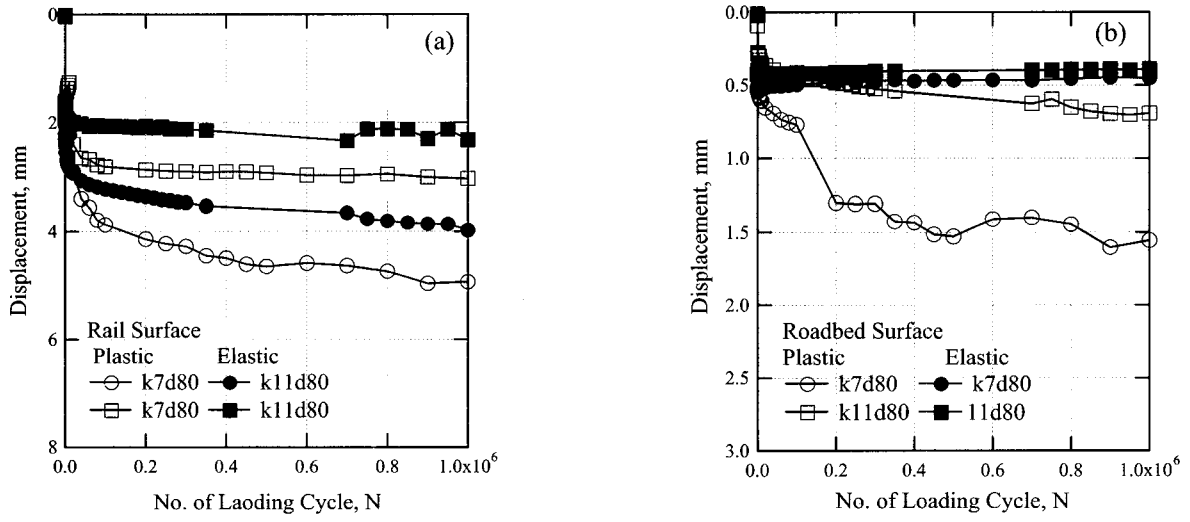

Fig 16. Relationship Between the Subgrade Reaction Modulus and the Plastic and Elastic Displacement of the Crushed Stone Roadbed Section

roadbeds were investigated through the real scale model test with the estimated actual train loads including impact load which is dependent on the train speed. The final conclusions are as follows:

(1) The load distribution and the displacement distribution in the test model with 5 sleepers were similar to the actual track condition.

(2) The plastic and elastic displacements of crushed stone roadbed section are always less than that of weathered granite soil roadbed section if the subgrade reaction moduli of both roadbed sections are the same with each other. The plastic displacement at the roadbed surface of both roadbed sections occurs rapidly at initial loading stage and converges to certain values after approximately 200 thousands loading cycles.

(3) The subgrade reaction modulus is a more important factor to the total plastic displacement of the track than the thickness of the crushed stone roadbed.

(4) The effect of roadbed thickness on the plastic and elastic displacement indicates that the magnitude of displacement in the roadbed layer tends to decrease with the increase of the thickness of roadbed.

References

1. E. T. Selig and J. M. Waters, "Track Geotechnology and Substructure Management", Thomas Telford.
2. Hwang, S. K., Lee, S. H., Choi, C. Y. and Lee, I. H. (2001), "Characteristics of Behavior of the Crushed Stone Reinforced Roadbed Under Cyclic Loading", *Proceedings of the KGS Spring 2001 National Conference*, Korea, pp.525-532. (in Korean)
3. Muramoto, K. and Sekine, E. (1998), "A Study on the Compaction Control of Embankments to Receive Train Loads", RTRI Report, Vol.12, No.4. (in Japanese)
4. Sekine, E. and Muramoto, K. (1995), "Bearing Capacity of Actual Existing Roadbed", RTRI Report Vol.9, No.7, pp.19-24. (in Japanese)
5. Sunaga, M. and Sekine, E. (1991), "A Study on the Development of Economical Reinforced Roadbed", RTRI Report, Vol.5, No.10, '91. 10., pp.25-33. (in Japanese)
6. William, F. A. (2000), "Model Testing of Two-Layer Railway Track Ballast", *Journal of Geotechnical Engineering and Geoenvironmental Engineering*, Vol.126, No.4, pp.317-323.

(received on Jun. 22, 2003, accepted on Feb. 27, 2004)